P01

微小重力下での多孔質媒体中の水分移動の機構解明

○渡邉幸，登尾浩助，小宮秀次郎，名倉理紗，鈴木心也（明治大学）

Elucidation of Water Flow in Porous Media under Microgravity

Yuki WATANABE, Kosuke NOBORIO, Shujiro KOMIYA, Risa NAGURA, Shinya SUZUKI (Meiji University)

1. Background and Objectives

To achieve a long-term mission with many crews, space farming has attracted attention over the years. Investigating water flow in porous media under space environments is one of the most important subjects to design space utilization from the viewpoints of hydrology, agriculture and civil engineering. However, because the space has different environments from the earth, the laws of water flow on the earth may not be valid in space. For example, water in soil flows according to Darcy's law on earth. But, in space, it may not be true. When we consider that the space used as agricultural land (such as on Mars or in a big spaceship, for example), understanding water flow in porous media under space environments is critical. Thus, the objective of our study was to elucidate the mechanism of water flow in porous media under microgravity.

2. Materials and Methods

We conducted a two-day parabolic flight experiment. Glass beads (GB) were used as porous media. We packed glass beads (6.3-6.9, 11, 20, and 30mm in dia., respectively) into transparent acrylic columns. Then, fluorescent aqueous solution was added to the columns, and the flow of the solution was visualized using black-light. We filmed the solution flowed with a video camera (SONY/HDR-CX700V).

To evaluate the water flow recorded with the video camera, we verified the surface wettability by measuring contact angles between the fluorescent aqueous solution and the wall of columns, and the surface of GB.

3. Results and Discussion

Wettability of the fluorescence solution on a column surface was larger than that on the GB surface. Due to the influence of wettability, water rose more preferably along the side wall of the columns than the void space of the GB. In this experiment, although we visualized water flow of the entire columns filled with GB, in the future, it is necessary to observe water flow in a void space with a smaller scale under microgravity.

Acknowledgments

This research was partly supported by the 9th students contest of microgravity experiments using an aircraft sponsored by JAXA.

P02

微小重力下での光ピンセットによる懸垂液滴径の計測

佐藤政史，○引地悠太，瀧本理仁，中谷辰爾，津江光洋（東京大学），今村宰（日本大学）

Measurement of Droplet Diameter Suspended by Optical Tweezers under the Microgravity

Masashi SATO , Yuta HIKICHI †, Rihito TAKIMOTO, Shinji NAKAYA, Mitsuhiro TSUE(The University of Tokyo) and Osamu IMAMURA (Nihon University)

1. Introduction

Optical tweezers enables to fix a free droplet spatially. Under microgravity, the capture force of optical tweezers becomes more effective due to no existence of gravity force and there is a possibility that this method will be strong tool for experiments of droplet vaporization and combustion. In this study, water droplets were suspended by optical tweezers in microgravity and the diameters of them were measured.

2. Experiment apparatus

Microgravity condition was made by parabolic flight which can make it for about 20 seconds. Laser beam was expanded and gathered to one point by microscope lens. Water droplets which were generated by nebulizer captured to the point. A CCD camera was directed to the point in order to record the images of the interference fringes.

The diameter of the droplets was calculated by the interometic particle imaging method from only parameters of the optical system and the number of interference fringes.

The similar experiment in normal gravity was done and used to compare effects of gravity level.

3. Results

The images of interference fringes were observed in the experiment. It shows that Suspensions of the droplets were succeeded in microgravity. From the interference fringes, the diameters of the droplets were calculated. The average of the diameters measured in microgravity was approximately 70 μm, on the other hand, that measured in normal gravity was 10 μm.

4. Conclusion

Water droplets suspended by optical tweezers were observed. The diameters measured in microgravity were larger than that measured in normal gravity.

References

1) IMAMURA Osamu, CHEN Bo, TSUE Mitsuhiro , Proceedings of the Forty-Seventh Symposium (Japanese) on Combustion: 190-191(2009)

P03

微小重力下における水時計と砂時計

○野中杏菜，八木澤唯，関口輝世，横田万里亜

Waterglass and Sandglass under the Microgravity

Azuna NONAKA, Yui YAGISAWA, Teruyo SEKIGUCHI, Maria YOKOTA

1. Experiment Overview

We perform a series of experiments on a sandglass under microgravity: we observe how granular materials behave differently inside a hopper under environments with reduced gravity. Granular materials are pressed each other under the gravity[1]. In this time the force in sands is through on chains[2]. It is said that granular materials have "viscosity"[3].

This state is like a solid state of molecular. When gravity is canceled by the flow of air from under the granular materials, the granular materials behave like fluid[1]. In other words, granular materials behave sometimes like liquid but sometimes like solid. As expected the behavior of granular medium inside the hopper tends to be more liquid-like under smaller gravity. In addition, we replace grains with liquid to see how the dynamics changes. Due to the stronger effect of capillary force under microgravity, as expected, the liquid tends to spread on the surface of the hopper. We vary the viscosity of liquid to see how inertia competes with viscosity dynamics qualitatively

2. Summary

We confirmed a close analogy between the behavior of granular material and that of fluid. As for liquid, if a shape of the container is unusual like a hopper, the phenomena are explained by considering effect surface tension [4].

3. Acknowledgments

We would like to express our gratitude to
Japanese Aerospace Exploration Agency,
Japanese Space Forum,
DIAMOND AIR SURVICE and
Dr. Ko OKUMURA, professor of Ochanomizu University.

References

1) Yoshihiro TANAKA: Sunadokei No Nanahushigi, Tyukyo Shinsho, 1996
2) J.Duran: Sand, Powders and Grains　An Introduction to the Physics of Granular Materials
3) Detlef Lohse, Devaraj van der meer: Nature, Vol.**459**,(2009)
4) P. Doshi and I.cohen, W.W.Zhang, M.siegel, P.Howell, O.A.Basaran, S.R.Nagel: Science, Vol.**302**, 1185,

P04

過重–微小重力下におけるオジギソウの挙動観察

○佐々木雄作，岩田ちひろ (岐阜大学)

Parabolic Flight Induced Alteration of the Behavior in Mimosa

Yusaku SASAKI, Chihiro IWATA (Gifu Univ.)

1. Introduction

Mimosa has a characteristic that its leaf is closed by contact with finger and then tilt down like a bow. This mechanism is that the contact-induced electrical signal stimulate the pulvinus, water moves to the trunk, and then turgor pressure is decreased. The water shift is depended on the gravitational direction, indeed, if the mimosa is set inverted, the leaf tilts up by contact.

Thus, we hypothesized that the contact-induced leaf movement might be altered during parabolic flight, i.e., the leaf tilts down by contact during hypergravity phase (≒2G), while tilt up might be observed during microgravity phase. In order to examine this hypothesis, we observed how gravity concern with this water movement by parabolic flight.

2. Method and Analysis

We observed behavior of mimosa by touching the leaf and branch during μG and hypergravity. We recorded its state by the video camera.

We compere the movement of mimosa in μG or hypergravity with in 1G by angle, angular velocity, etc.

There are some points to noted in this experiment. In low temperature, the sensitivity of mimosa to touch is decreased. So, we warm the rack in advance. And to prevent the dirt floating, we covered the pot which the mimosa stands in by a plastic cap.

3. Result and Discussion

In μG and hypergravity, the mimosa moved. But there are similar points and different points compered with movement in 1G. In concrete, the movement angle and the angular velocity in μG are similar to the movement of 1G. From this result, we can interpret that we could observe the pure movement of mimosa without one's own weight, and the mimosa have the mechanism that can make a specific change of turgor.

The other side, in hypergravity, the movement angle is larger and the angular velocity is little faster than its of 1G. This is because the brunch slackened off by one's own weight which doubled by 2G.

4. Acknowledgement

I am deeply grateful to Prof. Morita and Prof. Abe (department of Physiology Gifu University School of Medicine) , JAXA, JSF and DAS.

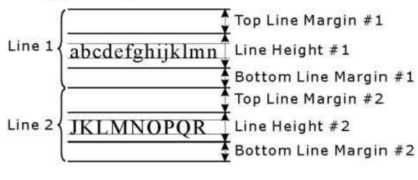

Fig. 1　This is a sample of a figure

干渉光学系を用いた原子輸送物性の測定

○金杉聡士，正木匡彦（芝浦工大）

Measurement of Atomic Transport Properties by using the Interferometer

Satoshi KANASUGI, Tadahiko MASAKI (Shibaura Institute of Tech.)

1. Introduction

The atomic transport properties in liquids are important subjects for the materials science in microgravity. The concentration distribution of solvent in the transparent materials can be observed by using interferometer. In this study, the diffusion coefficient and soret coefficient of aqueous solution of salts was studied by using interferometer as the ground-based research towards the microgravity experiment in the future.

2. Experimental Method

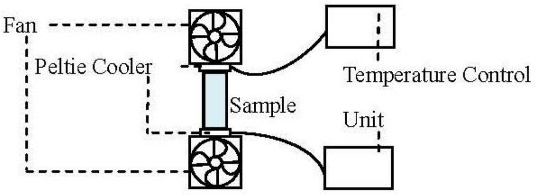

Fig.1 To the method of controlling the temperature of the sample

The normal Mach-Zehender interferometer was used for the measurement of diffusion phenomena. The aqueous solution of salts was contained in the square pillar cell(10mm x 10mm x 45mm) and fixed at the optical path of interferometer. **Fig. 1** shows the temperature control system, which was consisted of the Peltie cooler, cooling fan, current source, and micro computer. This system can make not only the isothermal condition but temperature-gradient condition.

3. Experimental Result

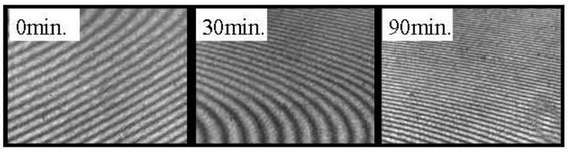

Fig.2 Time variation of the interference fringes due to the temperature gradient

The **Fig. 2** shows the time dependence of the fringe pattern of aqueous solution of salt in the temperature gradient condition.

The temperature of higher part of cell was 10 K higher than that of lower part of cell. The interval of fringes depends on the temperature gradient and concentration distribution of solution. The soret coefficient can be deduced from the progress of concentration distribution. The results will be presented in the poster session.

P06

静電浮遊法を用いた新たな熱物性計測法の開発

○梅山浩樹、正木匡彦

Development of a New Method of Thermophysical Properties Measurements by using the Electrostatic Levitator

Hiroki UMEYAMA , Tadahiko MASAKI

1. Introduction

The purpose of this study is the development of a new method for measuring thermophysical properties by using the electrostatic levitator. Nevertheless, the electrical properties, such as the electrical resistivity, is one of the most important properties of metallic melts at the extremely high temperature, the experimental data with sufficient accuracy have not been provided because of the experimental difficulties. The levitation technique together with the sample rotation by the induced magnetic field can be applied to the measurement of electrical resistivity. The rotation speed is the important factor for the measurement of electrical resistivity by this method, and usually, it can be measure by the observation of time dependency of reflection of rotating sample. However, in the case of sample with clean surface, the reflection intensity of rotating sample is constant. It makes difficult to the measurement of electrical resistivity. In this study, we develop the new method for the measurement of rotation speed of levitating sample by using the electrical resistivity together with a pulsed laser heating.

2. Experimental Apparatus

The spherical sample whose diameter was 2 mm was levitated by using the electrostatic levitation method. Four electromagnets were fixed around the sample to apply the rotational force of sample. The sample was heated by CO2 Lasers which were irradiated from the horizontal direction. The sample temperature was measured by single color pyrometers. The high power pulse laser was added to the system to make the spot whose temperature was higher than other area on the rotating sample. When the area faced to the pyrometer, the pulse-like signal was detected in the time dependence of sample temperature. Therefore, the frequency of sample rotation can be measured from the signal of pyrometers. The schematic figure of this system was shown in **Fig. 1**. The result will be presented in the poster session.

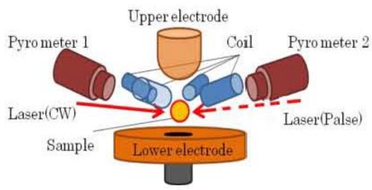

Fig.1 Schematic of the experimental apparatus

P07

ガス浮遊法とX線透過法を用いた金属液体の密度計測

○永江大輔，正木匡彦（芝浦工大）

Density Measurements of the Liquid Metals by using X-ray Transmission Method with a Gas Levitation Method

Daisuke NAGAE, Tadahiko MASAKI (Shibaura Institute of Technology)

1. Introduction

The gas-jet levitation method is one of the most powerful ways for keeping the molten metals with containerless condition. Nevertheless, the gas-jet have not been applied to the measurement of thermophysical properties because of observation difficulties. In this study, the x-ray transmission photography was combined with the gas-jet levitation method in order to observe the density of liquid metals.

2. Experimental

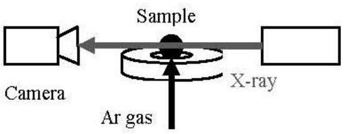

Fig.1 Schematic figure of apparatus

The spherical metal was levitated on the conical nozzle. The boron nitride was selected as the material of nozzle concerning the x-ray transparency. The x-ray source and CCD camera with x-ray image intensifier was fixed on the horizontal position of sample. The nozzle was contained in the chamber for the control of environment of sample. The schematic figure was shown in **Fig. 1**.

3. Result and Discussion

Fig.2 shows the x-ray transmission photographs of levitated samples whose diameters were 1.5mm, 2.0mm, and 2.5mm. The edge of shadows of spherical samples can be clearly observed and difference of diameters can be detected form the size of shadows. The volume of sample can be estimate from the curve fitting of shadow of sample. The experimental results and the accuracy of this measurement will be presented poster session.

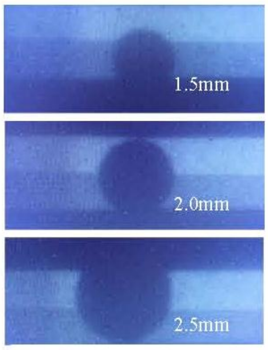

Fig.2 X-ray images of samples

P08

ハイブリッド両親媒性ポリマーによるW/Oエマルションの安定化：エマルション安定性とメカニズムの探究

○山﨑貴広（千葉科学大）、飯島聡、遠藤健司、酒井健一、酒井秀樹、阿部正彦（東京理科大）、
夏井坂誠（宇宙航空研究開発機構）、山下裕司、坂本一民（千葉科学大）

Stabilization of W/O Emulsions by Hybrid Amphiphilic Polymers: Exploration of Emulsion Stability and Its Mechanism

Takahiro YAMAZAKI (Chiba Instit. of Sci.),
Satoshi IIJIMA, Takeshi ENDO, Kenichi SAKAI, Hideki SAKAI, Masahiko ABE (Tokyo Univ. of Sci.),
Makoto Natsuisaka (JAXA), Yuji YAMASHITA, Kazutami SAKAMOTO (Chiba Instit. of Sci.)

We have developed a hybrid amphiphilic polymer (AIM-FN) consisting of a silicone backbone modified with hydrocarbon chains and hydrolyzed silk peptides. AIM-FN is molecularly soluble neither in water nor in most of organic solvents, but is attractive with these solvents due to its amphiphilic nature. This property enables the polymer to form "an independent third phase" being located at a silicone oil/water interface (**Fig. 1**), and hence, the emulsions are stabilized effectively based on a fundamentally distinguishable mechanism from the approach by conventional surfactants.

The size of the emulsion droplets prepared with AIM-FN is ca. 1 μm, independently on the composition in the stable water-in-oil (W/O) emulsion region. This W/O emulsion has long kinetic stability: coalescence hardly takes place, although creaming and flocculation are operative. Thus, the water droplets in the emulsion can be redispersed by a weak energy input.

The mechanisms of emulsion stability and deterioration still remain unspecified since the several physical processes are concertedly involved in the emulsion life-time under the gravitational environment. In this study, we focused on Ostwald ripening, one of the destabilized mechanisms of emulsion, and investigated the effect of the particle size of the dispersed phase on the emulsion stability in the water/AIM-FN/cyclic silicone oil (D5) system. The newly developed equipment (FILMIX® type40-40, PRIMIX Co.) can successfully provide well monodispersed water droplets in the emulsion. The particle size of this emulsion keeps constant for at least one week, bringing one a key outlook in terms of the emulsion stability principle.

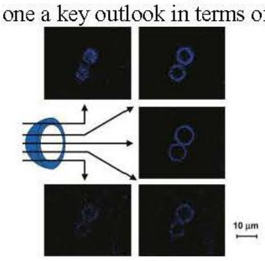

Fig. 1 CLSM images of W/O emulsion droplets with fluorescence-labeled AIM-FN.

P09

微小重力場における電線被覆上燃え拡がり火炎の消炎限界に対する芯線の役割

○髙橋修平，伊東弘行，中村祐二，藤田修（北海道大学）

Effect of Conductor on Extinction Limit of Spreading Flames over Wire in Microgravity

Shuhei TAKAHASHI, Hiroyuki ITO, Yuji NAKAMURA , Osamu FUJITA (Hokkaido Univ.)

For fire safety in space, the flammability of wire should be widely understood. However, it has not been examined well enough despite the high potential of causing fire in a spacecraft. We focused on a role of the conductor (inner core metal), which is one of the important characteristics of wire, and examined its role on extinction.

In this study, tests with flames spreading over wire were performed at varying external opposed flow conditions ranging from 50 to 250 mm/s with applying currents to the wire (0.0 A-1.5 A). The tests were conducted at both 1g and μg which was attained by parabolic flight. The wire used in this study has Nickel-chrome core (as a model of conductor) with polyethylene as an insulator. The 1g test result is shown in **Fig. 1**, indicating that the limiting value of oxygen concentration monotonically increases with the increase of the external flow velocity. At the conditions above the line, the wire becomes flammable, however under the line, it becomes nonflammable. More importantly, as the applied current increases, the extinction boundary moves to lower oxygen concentration and the external flow velocity dependence on the extinction limit is less pronounced. The μg test result is shown in **Fig. 2**, indicating that the wire becomes more flammable than in 1g.

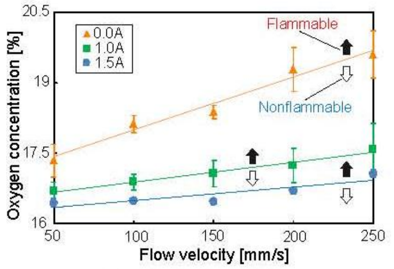

Fig.1 Extinction limit in 1g

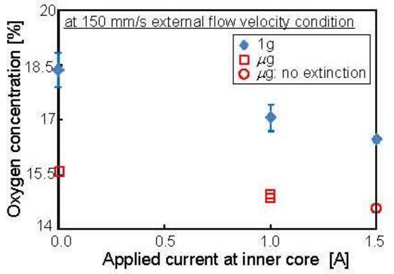

Fig.2 Extinction limit in 1g and μg at 150 mm/s external flow velocity (The square mark means that flame was sustained at that condition.)

P10

浮遊落下急冷法とドロップチューブ法を用いた Sm-Co 永久磁石材料の微細構造

○渡邊 陽、永山 勝久 （芝浦工大 工）

Permanent Magnetic Property and Microstructure of Sm-Co Alloys by using Melt Droplet Quenching and Drop Tube Process.

Akira WATANABE[1] , Katsuhisa NAGAYAMA[2]
[1]Graduate Student , Shibaura Institute of Technology
[2]Department of Materials Science , Faculty of Engineering , Shibaura Institute of Technology

We have investigated the permanent magnetic property and microstructure of samples of Sm_2Co_{17} and $SmCo_5$ alloys by using melt droplet quenching process and drop tube process.

Fig.1 shows the M-H loop of samples by using melt droplet quenching process .In **Fig.1**, the coercive force,(Hc) was obtained 2.6KOe(a), 1.6KOe(b) and 3.4KOe(c). High Hc sample was depend on the melt quenching effect in the melt specially.

Fig,2 shows SEM images of $Sm_{11.9}Co_{62.0}Fe_{19.2}Cu_{6.7}$ sample (Sm_2Co_{17} type magnet) by using melt droplet quenching process.

The microstructure was consist of $SmCo_5$ particles into Sm_2Co_{17} matrix.

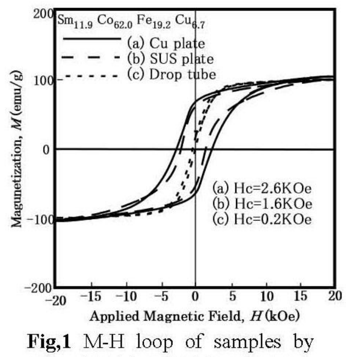

Fig,1 M-H loop of samples by using droplet quenching process

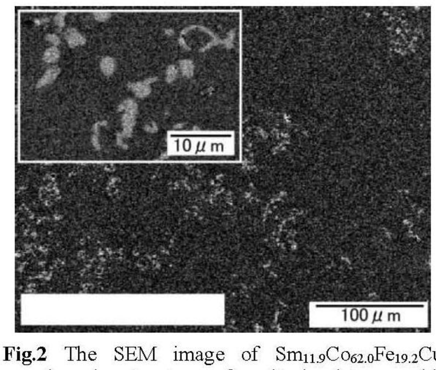

Fig.2 The SEM image of $Sm_{11.9}Co_{62.0}Fe_{19.2}Cu_{6.7}$ sample microstructure of melt droplet quenching process

電磁浮遊およびドロップチューブプロセスを用いた半導体 Si 中への 3dTM(Fe, Mn)添加に伴う過冷度と微細構造

○水谷優作, 永山勝久 (芝浦工業大学)

Undercooling and Microstructure of Added 3dTM(Fe, Mn) by using Electromagnetic Levitation and Drop Tube Process

Yusaku MIZUTNAI[1] and Katsuhisa NAGAYAMA[2]
[1]Graduate Student, Shibaura Institute of Technology
[2]Department of Materials Science, Faculty of Engineering, Shibaura Institute of Technology

We have many reported undercooling solidification, crystal growth and single crystal formation of Si by using electromagnetic levitation and short drop tube process.

In this study, we have expected the effect of levitation process for magnetic semiconductor creation that is expected to be a next-generation spintronics material in the future. Therefore, we conducted experiment with the addition of 3d transition metal(ferromagnetic and diamagnetic 3dTM) into Si by using short drop tube process. We have analyzed structure of the sample used by XRD, SEM-EDS, Laser microscope, EBSD in detail.

Fig.1 shows SEM image surface (a), (b) and microstructure (c), (d)[high undercooling sample: (a), (c) low undercooling sample: (b),(d)]. Sample surface structure (a) was shown fine dendrite growth and (b) was shown facet growth. α-$FeSi_2$ phase was formed at the grain boundaries in the sample (c), (d) especially.

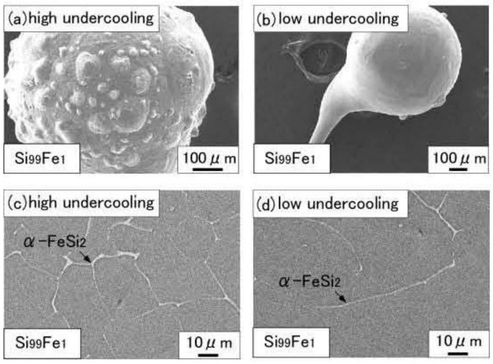

Fig.1 SEM image of surface and microstructure of $Si_{99}Fe_1$ used by drop tube process.

ショートドロップチューブプロセスを用いた Nd-Fe-B 磁石材料の高保磁力発現機構

○伊嶋 拓哉、永山 勝久 （芝浦工大 工）

The Mechanism of High Hc Properties in Nd-Fe-B Permanent Magnet by using Short Drop Tube Process

Takuya ISIMA[1] , Katsuhisa NAGAYAMA[2]
[1]Graduate Student, Shibaura Institute of Technology
[2]Department of Materials Science, Faculty of Engineering, Shibaura Institute of Technology

High coercive force of Nd-Fe-B is dependent on the interaction of the main phase and the grain boundary phase.

In this study, we have investigated high coercive force and formation of the ferromagnetic metastable phase to crystallize of wide range composition, $Nd_{71}Fe_{22}B_7$ (primary phase of α-Nd), $Nd_{67}Fe_{26}B_7$ (ternary eutectic), $Nd_{63}Fe_{30}B_8$ (primary of $Nd_2Fe_{14}B$) and $Nd_{59}Fe_{34}B_8$ (primary of $Nd_2Fe_{14}B$), by using short drop tube process.

Fig.1 shows hysteresis loops of $Nd_{71}Fe_{22}B_7$ (a), $Nd_{67}Fe_{26}B_7$ (b) and $Nd_{63}Fe_{30}B_8$ (c) samples. High coercive force, Hc, was obtained 4.6kOe (a), 4.5kOe (b) and 4.2kOe (c).

Fig.2 shows M-T corves of $Nd_{67}Fe_{26}B_7$ (b), $Nd_{63}Fe_{30}B_8$ (c) and $Nd_{59}Fe_{34}B_8$ (d) samples. All of samples, the Curie temperature was measured at 500 K. In this result, all of samples were not formed $Nd_2Fe_{14}B$ phase, especially.

We have discussed the formation of high Hc type metastable phase, in detail.

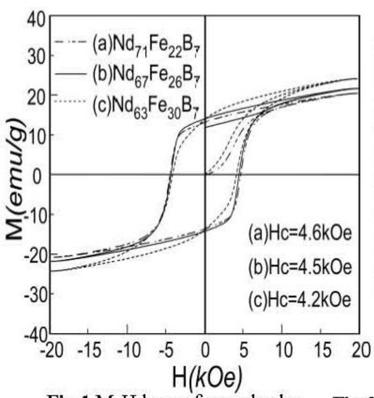

Fig.1 M-H loop of samples by using short drop tube process.

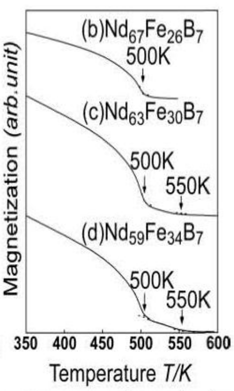

Fig.2 M-T corves of samples by using short drop tube process.

P13

過冷却融液からの凝固による p 型 Si-Ge 系熱電材料の合成

○濱田剛（横浜国大），永井秀明（産総研），奥谷猛（横浜国大）

Synthesis of p-type Si-Ge Thermoelectric Materials by Solidification from the Undercooled Melts

Tsuyoshi HAMADA (Yokohama National Univ.), Hideaki NAGAI (National Institute of Advanced Industrial Science and Technology), Takeshi OKUTANI (Yokohama National Univ.)

In previous studies, we found that the thermoelectric properties of Si-Ge could be improved by controlling structure using unidirectional solidification. For example, ZT to the growth direction of dendrites of Si-Ge solidified by unidirectional solidification became higher than that of the homogeneous Si-Ge. In this study, we improved the thermoelectric properties of p-type Si-Ge by an electromagnetic levitation (EML) method, because the containerless EML method is easy to obtain undercooling state in which the solidification rate is fast and directional solidification start from the point of trigger and the contact point of cooling gas.

The structures solidified from the melts with undercooling degrees of 77 and 187K were cells. The major axis of cell of sample solidified from melt with 77K undercooling was aligned with the direction of solidification. On the other hand, the structure of sample solidified from the melt with 187K undercooling was random cells. The rate of solidification of the melt with 187K undercooling was faster than that with 77K undercooling. Fast rate of solidification caused the random cellular structure because melt sphere was cooled from the surface of melt. Low rate of solidification caused the alignment of the major axis of cells with the solidification direction, because the solidification started at the point of trigger, the bottom of the melt sphere. The measurement results for the radial direction of this sample were found to exhibit lower thermal conductivity and higher electrical conductivity than that for the axial direction. Dimensionless figure of merit *ZT* was calculated as *ZT*=0.60 at 1100K (**Fig.1**).

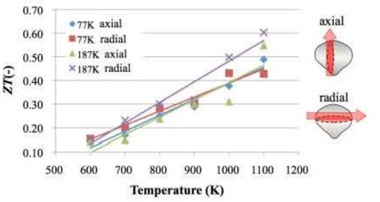

Fig.1 *ZT* for the axial and radial directions of $Si_{0.8}Ge_{0.2}$-1at%B solidified from various undercooling.

References

1) T. Okutani, Y. Kabeya, and H. Nagai: Preliminary Proceedings of Interdisciplinary Transport Phenomena Ⅶ : Fluid, Thermal, Biological, Materials and Space Sciences (ITP 2011), Dresden /Germany, (2011) pp.13-3.

P14

ドロップチューブ法を用いたウィスカー添加 La-3dTM-Al 系アモルファス微粒子生成に対する静的過冷却と落下無重力の効果

○吉岡　慎司、 永山 勝久 (芝浦工大 工)

Effect on the Static Undercooling and Microgravity for Amorphous La-3dTM-Al Fine Particles Formation Added Whisker by using Drop Tube Process

Shinji YOSHIOKA[1] and Katsuhisa NAGAYAMA[2]
[1]Graduate Student, Shibaura Institute of Technology
[2]Department of Materials Science, Faculty of Engineering, Shibaura Institute of Technology

We have many reported results, such as large undercooling behavior and amorphous formation ability increase for La system alloy added whisker by using a various electromagnetic levitation process.

In this study, we have investigated effect on the static undercooling and microgravity condition of the $La_{62}Al_{14}Cu_{12}Ni_{12}$ (at %) and sample added SiC whisker (0.5mass%) by using short drop tube process (free fall length :2.5m).

Fig.1 shows DTA curves of $La_{62}Al_{14}Cu_{12}Ni_{12}$ (a) and sample with added SiC whisker (0.5mass%) (b) by using drop tube process. These DTA curves were shown an exothermic peak due to crystallization of amorphous. In this figure, effectiveness of drop tube process in amorphous formation was shown. In sample (b) added SiC whisker, crystallization temperature T_{X1} shifted to the high temperature side and increased ΔT_X by SiC whisker addition. Stability of the amorphous local structure was increased to SiC addition, [sample (b)]. In this result was shown the local structure of amorphous alloy changed to the added SiC whisker. And we have considered effect on the static undercooling and microgravity condition.

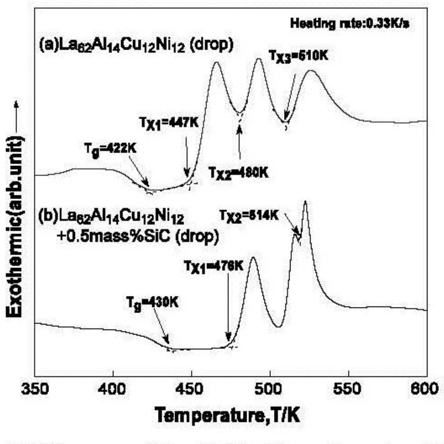

Fig. 1 DTA curves of $La_{62}Al_{14}Cu_{12}Ni_{12}$ and sample with SiC whisker addition (0.5mass%) by drop tube process

ドロップチューブを用いたZr-3dTM-Al系合金のアモルファス形成能に対する巨大過冷却の効果

○金山侑司，永山勝久　（芝浦工大　工）

Effect on the large undercooling of the amorphous formation ability in Zr-3dTM-Al system alloys by using drop tube process

Yuji Kanayama[1], Katsuhisa Nagayama[2],
[1] Graduate Student , Shibaura Institute of Technology
[2]Department of Materials Science , Faculty of Engineering , Shibaura Institute of Technology

We have many reported that RE-3dTM system alloys by using a various electromagnetic levitation and drop tube process. In this study, we have investigated the amorphous formation ability of $Zr_{65}Cu_{17.5}Ni_{10}Al_{7.5}$ quaternary system alloys by using the electromagnetic levitating melt droplet solidified into vacuum oil by used the new drop tube process.

Fig.1 shows the new drop tube system. The asymmetry coil was set in the vacuum chamber on the top of the short drop tube(free fall length 2.2m and oil depth 0.3m). The chamber was evacuated and then backfilled with He atmosphere. A spherical samples with 3~5mm in the diameter were levitated and melted by electromagnetic levitation apparatus force. Melted samples were dropped and solidified into the oil. This new process is different from the conventional drop tube process and possible to the fall condition without initial velocity. Solidifying the sample was caused static undercooling by dropped in the oil. We have discussed the amorphous formation ability about an effect of the microgravity and the static undercooling in detail.

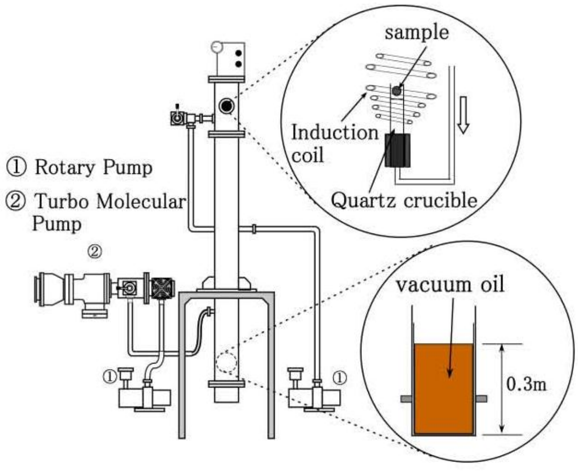

Fig.1 Schematic diagram of the new drop tube system

浮遊落下高速圧縮プロセスを用いたCu,Nb添加Pr-Fe-B系高性能永久磁石材料創製

○坂本 義徳、永山 勝久（芝浦工大）

High-performance permanent magnet creation Pr-Fe-B alloys added Cu and Nb by using the levitating melt droplet compression process

Yoshinori Sakamoto [1] , Katsuhisa Nagayama[2]
[1]Graduate Student , Shibaura Institute of Technology
[2]Department of Materials Science , Faculty of Engineering , Shibaura Institute of Technology

We have reported the magnetic anisotropy behavior using by electromagnetic levitating melt droplet compress ion process[1)]. In this study, quaternary melt that Cu and Nb added to the Pr-Fe-B alloy solidify the two plates in uniaxial compression for the purpose of creation the new type anisotropy high-performance permanent magnet materials.

Fig.1 shows M-H loops and SEM images of the melt droplet high-speed compression $Pr_{17}Fe_{76}B_7$ (a) and $Pr_{17}Fe_{76}B_{5.5}Nb_{1.5}$ (b) samples compacted by SUS304 plates. In Fig.1, M-H loops of the both samples were obtained large magnetic anisotoropy and high coercivity, Hc = 15kOe, especially. In sample (b), which was shown the loop of magnetic single phase state. Furthermore, the samples compacted by SUS304 steel 10 degree tilt was obtained significantly low coercivity 1.8kOe. In this result, the magnetic anisotropy was obtained by this high-speed compression process.

Microstructures of sample (a) and (b) were composed $Pr_2Fe_{14}B$ grain size about 1μm, which is surrounded by Pr-rich phase I . But in sample (b), in addition to these phases, it was composed Pr(Nb)-rich phase II , was contained Nb elements.

In this result, we have achieved creation of high-performance permanent magnet materials by using the melt droplet High-speed compression process

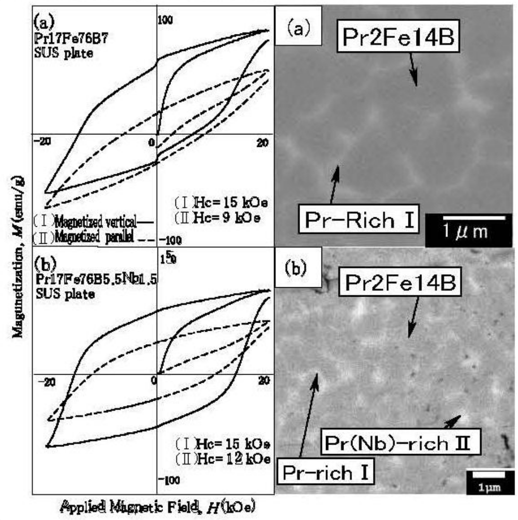

Fig.1 M-H loop and SEM image of compression samples compacted by SUS304 plates

1) K. Nagayama and Y. Sugita: Patent No. 2009-202163(2009.9.2)

P17

ドロップチューブで無容器凝固させたNd-Fe系非平衡相の高保磁力発現に対する3d-4f電子間結合の解析

○佐渡 拡行, 永山 勝久（芝浦工大）

The Analysis of 3d-4f Exchange Coupling State in Nd-Fe High Hc Type Metastable Phase by using Short Drop Tube Process

Hiroyuki SADO[1] , Katsuhisa NAGAYAMA[2]
[1]Graduate Student , Shibaura Institute of Technology
[2]Department of Materials Science , Faculty of Engineering , Shibaura Institute of Technology

We have many reported undercooling solidification behavior and high coercivity of Nd-Fe based metastable phase by using containerless process.

However, it is not clear about the mechanism of metastable phase formation and high coercive force.

$Nd_{33}Fe_{67}$ (Laves phase, RTM_2) and $Nd_{79.5}Fe_{20.5}$ (eutectic composition) alloys were solidified by using short drop tube apparatus (free fall length 2.5m). These samples were analyzed by vibrating sample magnetometer (VSM), differential thermal analysis (DTA) and scanning electron microscopy (SEM).

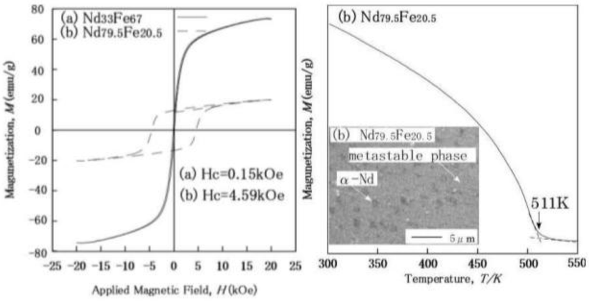

Fig.1 M-H loop of Nd-Fe samples and M-T curve with SEM image of $Nd_{79.5}Fe_{20.5}$ sample

Fig.1 shows the M-H loops of $Nd_{33}Fe_{67}$ (a) and $Nd_{79.5}Fe_{20.5}$ (b) samples and M-T curve with SEM image of sample (b). Sample (a) was shown soft magnetism caused by Nd_2Fe_{17} phase but sample (b) was shown high coercivity. And M-T curve of sample (b) detected Curie temperature, Tc = 511K of Nd-Fe high Hc type metastable phase.

Therefore we investigated the relation between the mechanism of high coercive force and the interaction of 3d-4f exchange coupling state used by X-ray photoelectron spectroscopy (XPS) with these samples, in detail.

P18

$Nd_2Fe_{14}B$相のC軸配向と高保磁力発現に対する浮遊落下急冷凝固プロセスの効果

○坂本 一樹、永山 勝久（芝浦工大 工）

The Orientation of C Axis and High Hc Behavior of $Nd_2Fe_{14}B$ Phase by using Levitating Melt Droplet Quenching Process.

Kazuki SAKAMOTO (Graduate Student, Shibaura Institute of Technology)
Katsuhisa NAGAYAMA (Department of Materials Science, Faculty of Engineering, Shibaura Institute of Technology)

We have many reported the high coercive force behavior of Nd-Fe-B permanent magnet material by using containerless levitating solidification process.

In this study, we have examined the high coercive force of $Nd_{15}Fe_{77}B_8$ alloy by using levitating melt droplet quenching process. And we have investigated the flow of the melt, crystal growth and orientation of C axis in $Nd_{15}Fe_{77}B_8$ phase in detail.

Fig.1 shows the new levitating melt droplet quenching process. This process was levitated and melted a sample into the electromagnetic levitation asymmetrical coil, which was dropped and quenched on Cu plates (θ=0~45°) and Cu cylinders (φ=60~180mm).

Fig.2 shows XRD pattern of $Nd_{15}Fe_{77}B_8$ melt droplet quenching samples (θ=0°(a), θ=15°(b)). In figure, the sample (b) was measured the complete orientation of C axis.

In this result, it was suggested the orientation of C axis of $Nd_2Fe_{14}B$ phase were depended on the melt flow.

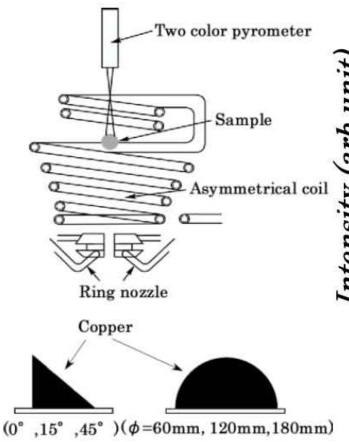

Fig.1 Schematic diagram of the new levitating melt droplet quenching process.

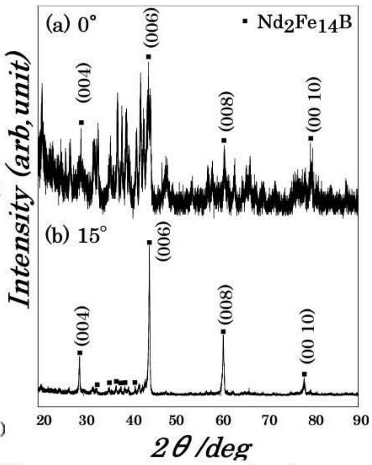

Fig.2 XRD pattern of $Nd_{15}Fe_{77}B_8$ melt droplet quenching samples on Cu plates.

浮遊液滴の回転分裂挙動を利用した粘性係数測定

○田中類比（筑波大院），松本聡（JAXA），金子暁子，阿部豊（筑波大学）

Viscosity Measurement using Breakup of Levitated Droplet

Rui TANAKA (University of Tsukuba), Satoshi MATSUMOTO (Japan Aerospace Exploration Agency),
Akiko KANEKO, Yutaka ABE (University of Tsukuba)

Thermophysical property measurement of material without container is promising technique with high accuracy for high temperature molten state. Levitation technique realizes the containerless processing even on the ground. The purpose of this study is to establish measurement technique of viscosity with moderate viscous range, which has no conventional measurement method. In this study, a droplet is levitated by electrostatic force, and induced to rotate. As angular velocity increased, the droplet finally broke up to two droplets. The shape just before breakup is shown in **Fig. 1**. The deformation differed depending on viscosity. By applying the principle of "Liquid Filament Rheometer (LFR)", which is viscosity measuring instrument by utilizing deformation of fluid column, to the breakup of levitated droplet[1], we derived eq. (1) to estimate viscosity.

$$\eta_c = \frac{\left(2mR\Omega^2 / \pi D_{mid}\right) - \sigma}{-3\left(dD_{mid} / dt\right)} \qquad (1)$$

where η_c, m, R, Ω, D_{mid}, σ are calculated viscosity, mass, length from middle to gravity center of the droplet, angular velocity, midpoint diameter, respectively. Each terms m, R, Ω, D_{mid} are measured directly, and σ is calculated by theory[2]. η_c calculated by eq. (1) is shown in **Fig. 2**. Thus it is suggested that viscosity of levitated droplet is measured by using breakup.

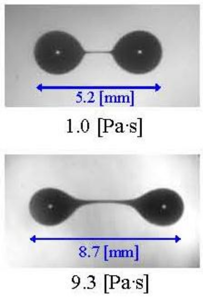

Fig. 1 Breakup of droplet

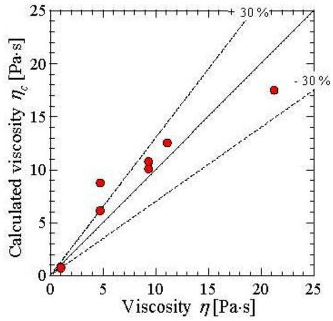

Fig. 2 Result of viscosity measurement

References

1) G. H. McKinley and A. Tripathi: J. Rheol., **44** (2000) 653.
2) D. D. Elleman, T. G. Wang and M. Barmatz: NASA Tech. Memo, **2** (1988) 557.

パラジウム合金膜を用いた二酸化炭素還元装置からの水素の回収

○長谷川智大，鈴木進補 (早稲田大学)，島明日香，桜井誠人，大西充（JAXA)

Collection of Hydrogen from Carbon Dioxide Reduction Apparatus Through a Palladium Alloy Membrane

Tomohiro HASEGAWA, Shinsuke SUZUKI (Waseda Univ.),
Asuka SHIMA, Masato SAKURAI, Mitsuru ONISHI (JAXA)

For manned space mission, CO_2 reduction apparatus is considered as the most important technique to maintain the life of the spaceship crews. In previous studies, an apparatus was developed to reduce CO_2 by H_2 using Ru catalyst through Sabatier reaction[1]. It was found that the gas from the outlet of the reactor contained unreacted H_2. Therefore, this study aimed to develop a device for collection of H_2 in the gas from the outlet using a molecular sieve made of a Pd-alloy membrane. We measured hydrogen permeation rate of the device at low temperatures to investigate the possibility of collection of H_2 for CO_2 reduction apparatus.

Figure 1 shows the experimental apparatus. Before the experiments the tubes are filled with N_2 gas to prevent oxidation of the apparatus. First, the tubes were evacuated and the mixture gas of CO_2 and H_2 was supplied from the gas cylinder and was flowed in a tube ($150 < T < 300$ °C, 100ml/min). Some amount of gas was permeated through a Pd-Cu membrane (15μm thick). The rest of the gas was flowed to another tube. The hydrogen permeation rate Φ of Pd-Cu was calculated using the flow rate and the composition of the rest gas. The composition of the rest gas was analyzed by gas chromatography.

The hydrogen permeation rate ($1.04\times10^{-9} < \Phi < 4.22\times10^{-9}$ molH_2/m·s·$Pa^{0.5}$) agreed with the literature[2] at low temperatures ($150 < T < 300$ °C). Therefore, this device can be used for collection of hydrogen to improve the efficiency of CO_2 reduction apparatus.

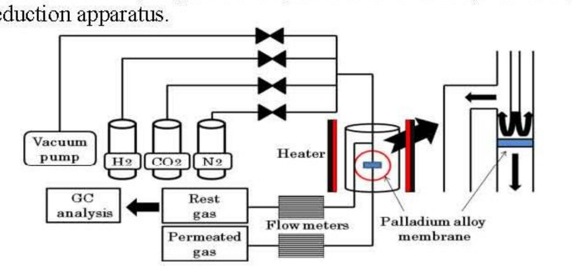

Fig.1 Schematic diagram for permeation test

Acknowledgment

TANAKA Kikinzoku kogyo K.K. Technical Division's support (Pd-alloy membranes, data, and discussion) was invaluable for this research.

References

1) Y.Ito, S.Suzuki, A.Shima, M.Sakurai, M.Onishi, JASMA, Vol.28 No.4, (2011) J19
2) TANAKA Kikinzoku kogyo K.K. Technical data

ホログラフィック光ピンセットを用いた二次元コロイド結晶の核形成制御

○仙波稔己（東北大学），石川正道（理化学研究所），塚本勝男（東北大学）

Nucleation Control of Two Dimensional Colloidal Crystal by Holographic Optical Tweezers

○Toshiki SENBA (Tohoku University), Masamichi ISHIKAWA (RIKEN), Katsuo TSUKAMOTO (Tohoku University)

1. Introduction

Colloidal crystal is a name of ordered structures composed of monodispersed colloids. It is thought that crystallization of colloidal crystals is caused by KirkWood-Alder transition because of the repulsive interaction. However, some phenomena that cannot be explained by the repulsive force only are observed in the colloidal dispersions under the conditions of low particle concentration and low ionic strength, void structure and gas-liquid phase separation. These phenomena suggest the existence of a long-range attractive interaction between particles. To detect the long-range inter-particle interaction, we observed the dissolution process of colloidal crystal in solution.

2. Experiment

A colloidal particle can be controlled by the light pressure of condensed laser. Multi-particles can be arranged by using a spatial light modulator that can modulate the phase of light. We originally manufactured the holographic optical tweezers and conducted the dissolution experiment of colloidal crystal. The experimental procedure is as follows. 1 μm polystyrene particles were dispersed in a glass cell. The particles settled on the bottom of the cell after a while. We arranged the colloidal particles using the holographic optical tweezers to form an ordered cluster. Then, we observed the disordering due to the Brownian motion using optical microscope.

3. Result and Discussion

We succeeded in preparing an ordered cluster (**Fig.1**). After turning off the optical tweezers, the cluster began to disperse. We measured the position of each particle at moments to evaluate the degree of disordering. We found it turned out that the lifetime of the cluster depends on the salt concentration (**Fig.2**).

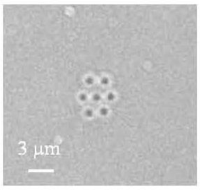

Fig.1 hexagonal cluster

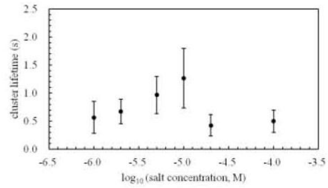

Fig.2 Cluster lifetime and salt consentration

シアーセル法を用いた液体 Sn-Pb 合金中の相互拡散係数測定

○鈴木浩嗣，山田紀幸，田中杏奈，鈴木進補（早稲田大学）

Measurement of Interdiffusion Coefficient of Liquid Sn-Pb Alloy by using the Shear Cell Technique

Koji SUZUKI, Noriyuki YAMADA, Anna TANAKA, Shinsuke SUZUKI (Waseda Univ.)

Although the validity of Darken's equation was confirmed in diffusion mechanism of crystal, the validity of the equation has not been revealed in the liquid. This study aimed to investigate the validity of Darken's equation in liquid by comparing interdiffusion coefficient obtained by Darken's equation with experimental value.

We measured interdiffusion coefficient in liquid Sn and Sn-10at%Pb alloy by using the FOTON shear cell technique and stable density layering. The diffusion temperature was 773K and the diffusion time was 12600s. After diffusion experiments, we obtained 20 divided specimens, and measured Sn and Pb concentrations with ICP-OES. Concentration profiles of Pb were obtained by dividing the measured Pb concentration by the sum of both Pb and Sn concentrations. The obtained concentration profiles were fitted by the semi-infinite layer solution. Interdiffusion coefficients were determined through the corrections for the shear convection and averaging effect.

The semi-infinite layer solution fitted the Pb concentration profile (**Fig. 1**) well with a high coefficient of determination r^2=0.997. The obtained interdiffusion coefficient by fitting was 3.91×10^{-9} m^2/s. On the other hand, the interdiffusion coefficient D of 3.85×10^{-9} m^2/s was obtained by Darken's equation (eq.(1)) [1] using the following values.

$$D = (D^*_{Sn} \times N_{Pb} + D^*_{Pb} \times N_{Sn})(1+\frac{d\ln\gamma_{Sn}}{d\ln N_{Sn}}) \quad (1)$$

Here N_{Sn} (=0.95) and N_{Pb} (0.05) are atomic fractions of each element: D^*_{Sn} and D^*_{Pb} are selfdiffusion coefficients [2]: and γ_{Sn} is activity coefficient of Sn at the particular concentration.

The relative difference ΔD/D between the value obtained by Darken's equation and the experimental value was 1.3%.

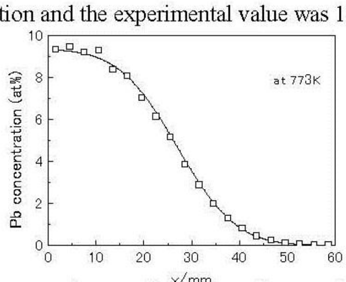

Fig.1 Pb concentration profile against distance from the end of the capillary. The system was Sn-10at%Pb versus Sn.

References

1) L. S. Darken, Trans. AIME, **175**, (1948), 184-194.
2) G. Frohberg, J. Non-Cryst. Solids, **205-207**, (1996), 412-416.

2 波長マッハツェンダー干渉計による熱拡散係数の測定

○橋本栄尭，森雄飛，鈴木進補 (早稲田大学)，稲富裕光 (JAXA)

Measurements of the Soret Coefficients with Two-Wavelength Mach-Zehnder Interferometer

Yoshitaka HASHIMOTO, Yuhi MORI, Shinsuke SUZUKI (Waseda Univ.), Yuko INATOMI (JAXA)

Soret effect (thermal diffusion) plays an important role in solidification and crystal growth processing operations. Therefore, development of measurement method for Soret coefficients with high accuracy is required. This study aimed to establish a measurement method for temperature and concentration distribution during Soret experiments using two-wavelength Mach-Zehnder interferometer, which has been used for experiments of crystal growth[1]. We observed interference fringes generated through transparent solution samples to investigate the possibility of Soret experiments by this method.

Pure salol and salol-8mol% tert-butyl alcohol solution were set in a quartz sample cell. The cell was sandwiched between two Peltier devices and inserted in the interferometer (**Fig.1**). At first, both top and bottom sides of the cell were heated at 65 °C with Peltier devices to melt the sample. After the temperature of samples became homogeneous, the top and bottom sides were heated at 60 and 30 °C, respectively, so that the density increased toward the bottom side to suppress convection. Until the steady state, we counted the number of moving fringes which crossed a measuring point to calculate temperatures and concentration distributions. The state at the time when the position of the fringe did not change was defined as the steady state.

The time to reach the steady state of salol-8mol% tert-butyl alcohol was longer than that of pure salol. It is considered that the Soret effect caused by the concentration gradient was generated in salol-8mol% tert-butyl alcohol, but not in pure salol where no concentration gradient existed. The differences of the results between two wavelengths are the number of the fringes observed in a unit area and crossing the measuring point.

The two-wavelength Mach-Zehnder interferometer enables us to observe Soret effect and measure temperature and concentration distributions individually.

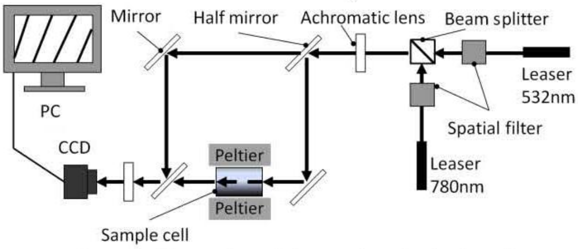

Fig.1 Schematic illustration of the Mach-Zehnder interferometer

References

1) Y. Inatomi, M. Ashida, K. Sakata, J. Wang, T. Okutani, J. Jpn. Assoc. Cryst. Growth, **39**, 1(2012)11.

超音波浮遊している溶融液滴の冷却凝固過程に関する研究

○下西国治，金子暁子，阿部豊 (筑波大学)

Study on Cooling Process of Acoustically Levitated Molten Droplet

Kuniharu SHITANISHI, Akiko KANEKO, Yutaka ABE (University of Tsukuba)

Container-less processing using levitation technique can prevent heterogeneous nucleation and contamination due to the container wall. Thus, it is expected to be used in analytical chemistry and production of new materials under microgravity environment. Acoustic levitation is one of the levitation techniques. It shows nonlinear and unsteady behavior. For example, internal flow, external flow, deformation and oscillation. These behaviors could affect to cooling process of acoustically levitated molten droplet. Thus, the cooling process of acoustically levitated molten droplet is investigated in this present study.

Figure 1(a) shows the time series change of the surface temperature of the levitated droplet. The surface temperature drops after the levitation and when the nucleation starts, temperature rises to the melting point. Then, temperature drops again. **Figure 1**(b) shows the image of droplet at t = 4.3s when the nucleation starts. The nucleation of levitated molten droplet starts from side and then spread to the surface. After the solidification of the surface, solidification inside the droplet starts. **Figure 2**(a) shows the image and IR image which shows the surface teperature of the droplet at t = 50s. **Figure 2**(b) shows the surface temperature distribution in the vertical direction at the center of the droplet. From these figures, it can be said that liquid remains at the bottom of the droplet ever after 50s. This may be the effect of internal flow of the levitated droplet.

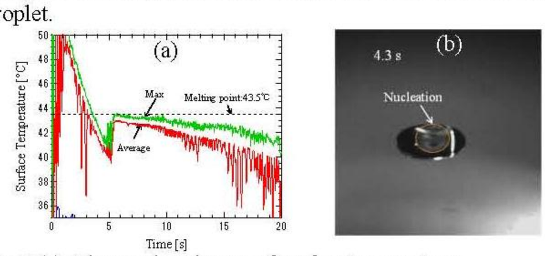

Fig.1 (a): Time series change of surface temperature.
(b): Image of the levitated droplet at t = 4.3s

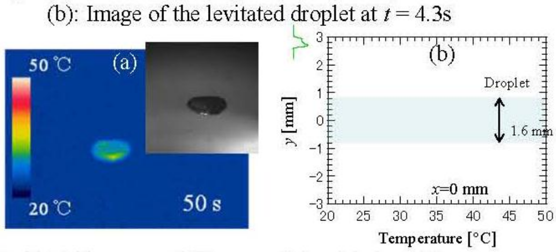

Fig.2 (a): Image and IR image of droplet at t = 50s
(b):Surface temperature distribution in vertical direction

温度差マランゴニ効果による懸垂液滴内粒子挙動と Hydrothermal wave 不安定性

○渡邉拓実，上野一郎 (東京理科大学)

Particle behavior and hydrothermal wave instability in hanging droplet due to thermocapillary effect

Takumi WATANABE, Ichiro UENO (Tokyo Univ. of Science)

We focus on thermocapillary-driven convection in a hanging droplet. We realize several flow patterns in the droplet by increasing the temperature difference between the sustaining rod and droplet tip by a series of experiments[1]. We have a transition of the flow field from a two-dimensional steady flow to three-dimensional time-dependent 'oscillatory' ones. The oscillatory flow is accompanied with a thermal wave traveling over the free surface at a constant frequency known as hydrothermal wave instability[2](HW).

In the present research, we evaluate the transition point of the flow inside the droplet, and the fundamental frequency of the oscillatory flow after the transition. We make a comparison of the present data with the ones by on-orbit experiments in the Japanese Experimental Module 'Kibo' aboard the International Space Station (ISS)[3].

References

1) T. Takakusagi, I. Ueno, and C. Hong, Bulletin European Low Gravity Research Association **27** (2010) 32.
2) M. K. Smith and S. H. Davis, J. Fluid Mech. **132** (1983) 11.
3) H. Kawamura, K. Nishino, S. Matsumoto, and I. Ueno, J. Heat Transfer **134** (2012), 295.

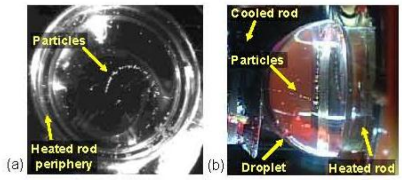

Fig. 1 Example of view obtained by one of the top view cameras (a) and side view camera (b) in on-orbit experiments (MEIS-3)

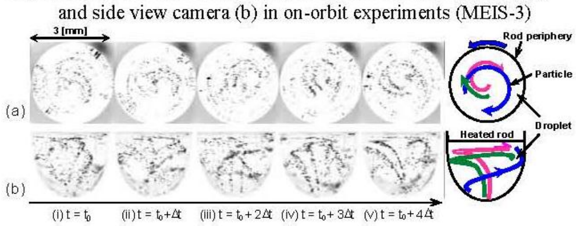

Fig. 2 Time series of snapshots of Dynamic PAS flow[1] at time interval Δt 0.117 [sec].Spatio-temporal correlation between particle line observed (a) from above and (b) from side respectively.

高プラントル数流体における液柱内マランゴニ対流不安定性への液柱サイズの影響

○大村洸平（筑波大院），松本聡（JAXA），阿部豊，金子暁子（筑波大学）

Size Effect on Instability of Marangoni Convection in Liquid Bridge with High Prantl Number

Kouhei OOMURA (University of Tsukuba), Satoshi MATSUMOTO (Japan Aerospace Exploration Agency),
Yutaka ABE, Akiko KANEKO (University of Tsukuba)

Marangoni convection is the flow driven by the presence of a surface tension gradient which can be produced by temperature difference at a liquid-gas interface. It is known that flow affects the quality of grown crystal by a Floating Zone (FZ) method. Half zone system is often employed to understand a nature of flow behavior as a simplified model[1)]. Two-dimensional steady flow transits to three dimensional oscillatory one at critical temperature difference between supporting disks. This transition condition is organized using critical Marangoni number.

The objective of this study is to investigate influence of size on the onset condition of oscillatory flow by comparing experimental results both under terrestrial condition and microgravity aboard the International Space Station.

Figure 1 is showed a schematic drawing of experimental apparatus on ground. A liquid bridge can be formed between cylindrical upper and lower disks of 10 mm in diameter. Thermocapillary flow is caused by imposing the temperature difference between disks using a DC power supply. The flow and temperature fields are observed by CCD camera and several fine thermocouples.

In the presentation, critical Marangoni number and oscillatory behavior of temperature is shown and the buoyancy and size effects are discussed.

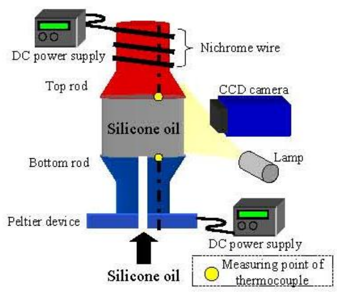

Fig. 1 Schematic of the experimental apparatus

Reference

1) H. Kawamura, K. Nishino, S. Matsumoto and I. Ueno: J. Heat Transfer, **134** (2012) 031005-1.

先行薄膜形成過程における含有粒子の影響

○日比野哲也(東理大学) 橋本翔太(東理大院) 上野一郎(東理大)

Effect of Suspended Particles on Precursor Film Formation ahead Spreading Droplet

Tetsuya HIBINO[1], Shota HASHIMOTO[2], Ichiro UENO[3,4]

[1]Undergraduate, Dept. Mechanical Engineering, Fac. Science & Technology, Tokyo University of Science
[2]Div. Mechanical Engineering, Graduate School of Science & Technology, Tokyo University of Science
[3]Dept. Mechanical Engineering, Fac. Science & Technology, Tokyo University of Science
[4]Research Institute for Science & Technology (RIST), Tokyo University of Science

In a case of complete wetting, a very thin film spreads ahead of the macroscopic edge of the droplet on a solid surface. This thin film is called precursor film. An example of applications of wetting and spreading of the droplet with suspended particles would be printed-wiring board using ink-jet technology. The purpose of this experiment is to show in effect of particles suspended in a droplet on the precursor film formation as well as the droplet spreading.

We apply the Brewster angle microscopy (BAM, hereafter) to detect the precursor film ahead of the macroscopic contact line (M-CL, hereafter) and to measure its existing length.

We compare the results of the experiments done on silicone oil in **Fig. 1**; (a) indicate results with the particles and (b) results without the particles.

In the poster, the authors will discuss the effect by considering the shape of the droplet in the vicinity of the M-CL and the precursor film formation.

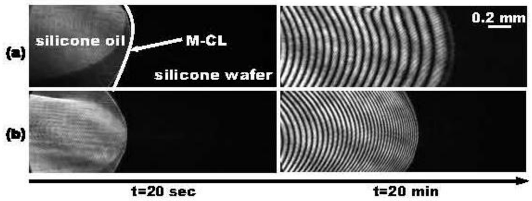

Fig. 1 Successive snapshots of precursor film in the case of 2-cSt silicone oil droplet with-particles **(a)** and without-particles (b) detected by BAM. The left figures indicates the beginning of dropping (t=0(min)) and right figures after 20min.

Acknowledge
This research was conducted as an activity of the International Research Division on Interfacial Thermo-Fluid Dynamics (I[2]Plus) in Research Institute for Science & Technology at Tokyo Univ. of Science.

金属融体の表面張力測定おける酸素ポンプの利用

○武井悠翔，小澤俊平（千葉工大），高橋優，渡辺直行（首都大），渡邊匡人（学習院大）

Employment of Oxygen Pump for Surface Tension Measurement of Molten Metals

Yuto TAKEI, Shumpei OZAWA (Chiba Institute of Technology),
Suguru TAKAHASHI, Naoyuki WATANABE (Tokyo Metropolitan Univ.),
and Masahito WATANABE (Gakushuin Univ.)

1. Introduction

Electromagnetic levitation (EML) enables us to measure surface tension of molten metals over wide temperature range including undercooling condition. Furthermore, it is easy to control oxygen partial pressure (Po_2) of atmospheric gas, which strongly influences on surface tension of molten metals. However theoretically-derived Cummings and Blackburn equation[1)] is required for the calibration of the droplet deformation due to the gravitational acceleration and magnetic force from a levitation coil when this technique is employed on the ground. In order to prove the validity of the Cummings and Blackburn calibration, a long period microgravity experiment without any gravity change is expected at the International Space Station (ISS).

In this study, a zirconia oxygen pump was employed to control oxygen partial pressure of atmospheric gas during surface tension measurement of molten nickel by EML. The purpose of this study was to investigate the effectiveness of the oxygen pump for the microgravity experiment on surface tension measurement.

2. Result

The temperature dependence of the surface tension of molten nickel exhibited a kink due to competition between the temperature dependence of oxygen partial pressure and that of the oxygen adsorption equilibrium constant as in the case of the surface tension measured under reducing gas atmosphere of Ar-He-5 vol. %H_2. Even though the Po_2 is different between these experiments, almost the same surface tension is observed at low temperature. The result of surface tension measurement implied that the influence of dissociation of H_2O should be considered for accurate evaluation of oxygen partial pressure of atmospheric gas prepared by oxygen pump

References

1) D. L. Cummings and D. A. Blackburn; J. Fluid Mechanics, **224**, (1991) 395.

宇宙実験における熱電対による温度測定システムの小型化と高精度化

○林田貴大，馬場宗明，廣川智己（九州大学），栗本卓(JAXA)，新本康久，大田治彦（九州大学），
浅野等（神戸大学），河南治（兵庫県立大学），鈴木康一（山口東京理科大学），
今井良二（株式会社 IHI），川崎春夫，駒崎雅人，松本聡，藤井清澄(JAXA)

Development of Compact and Accurate Temperature Measurement System for Space Experiment

○Takahiro HAYASHIDA, Soumei BABA, Tomoki HIROKAWA (Kyushu Univ.), Takashi KURIMOTO (Japan Aerospace Exploration Agency), Yasuhisa SHINMOTO, Haruhiko OHTA (Kyushu Univ.), Hitoshi ASANO (Kobe University), Osamu KAWANAMI(University of Hyogo), Koichi SUZUKI (Tokyo University of Science, Yamaguchi), Ryoji IMAI (IHI Corporation), Haruo KAWASAKI, Masahito KOMASAKI, Satoshi MATSUMOTO, and Kiyosumi FUJII (Japan Aerospace Exploration Agency)

1. Introduction

Downsizing of experimental apparatus and dense packing for the effective use of available rack volume are required in the experiments onboard ISS. For two-phase flow (TPF) experiments in Japanese space platform KIBO, a temperature measuring system is developed to minimize the volume of the system. To clarify the flow boiling phenomena under microgravity conditions, the measurement of heat transfer coefficient and critical heat flux is an important objective. To compare the results from the reference experiments conducted separately on ground, the measurement of temperature data with high accuracy becomes a key. For the temperature measurement by using thermocouples, however, the employment of a cold junction compensator commercially available is impossible in microgravity experiments because of its structure using temperature-controlled liquid reservoir. Development of a method for reliable cold junction with uniform temperature for all thermocouples is required to obtain the temperature data with an error less than 0.3K.

2. Technique for temperature measurement using thermocouples in orbit

The present study discusses about the following subjects.

i) Wiring patterns of circuits for accurate temperature measurement
ii) Conversion from electromotive forces (EMF) to temperatures
iii) Structure for cold junctions exposed to ambient temperature

References

1) K. Fujii et al., Proc. 28th International Symposium on Space Technology and Science, 2011-h-30, 2011

非共溶性混合媒体の核沸騰における熱伝達特性の改善

○大西俊輔，大谷伸生，小林寛幸，大田治彦（九州大学）

Boiling Heat Transfer by Nucleate Boiling of Immiscible Liquid

Shunsuke ONISHI, Nobuo OHTANI, Hiroyuki KOBAYASHI, Haruhiko OHTA (Kyushu Univ.)

By developments of electronic technology, a heat generation density from semiconductors is growing. On the other hand, electronic devices of Si semiconductors have a restriction of operating temperature. New semiconductors of SiC or GaN with higher thermal toughness are still under development especially those of large capacity. The cooling of large semiconductors such as power electronics with high heat generation density becomes an important problem. Boiling and two-phase flow is expected as one of the most effective methods to cool the electronic devices because of its superior heat transfer characteristics. The present research concentrates on the selection of coolant, i.e. immiscible liquid mixtures. Most of the existing researches on nucleate boiling of binary mixtures clarify the heat transfer characteristics peculiar to the miscible ones, while the studies for immiscible mixtures were very limited. In this paper, we concentrated on the possibility of immiscible liquid mixtures in nucleate boiling heat transfer.

Pool boiling experiments on nucleate boiling of immiscible liquid mixture are performed in a closed vessel at 0.1MPa. The immiscible liquid mixture consists of more volatile component with a higher density and less volatile component with a lower density and we select FC72/Water, Novec649/Water and Novec7200/Water. The experimental data is acquired under the steady-state conditions at heat flux ranging from those for the boiling incipience to CHF or to the highest possible heat flux under the restriction by the experimental setup. Before the experiments, the heights of liquid layers for both components on the horizontal heating surface before the heating are kept at constant, and the thickness of layer for more volatile component with a higher density above the heating surface is varied as an important parameter.

When the thickness of more volatile component with a higher density is very small, a new phenomenon of “intermediate burnout” is observed. At heat flux higher than that for intermediate burnout, the immiscible mixture decreases the surface temperature from that for pure water under the constant pressure condition and simultaneously increases CHF. The increase of CHF is expected to be due to the high subcooling of less volatile component resulted from the pressurization by the vapor pressure of more volatile component. The immiscible mixture has a potential to realize high performance heat exchange systems by the self-sustaining subcooling of components even for a closed system.

微小重力条件下における核沸騰熱伝達特性に及ぼすサブクール度および残留重力の影響

○福山雄太，金澤昇平，永安忠，新本康久，大田治彦（九州大学），　河南治（兵庫県立大学），
Oleg KABOV，Sergey CHIKOV（ロシア科学アカデミー），Queeckers PATRICK（ブリュッセル自由大学），
Johannes STRAUB（ミュンヘン工科大学）

Effects of Liquid Subcooling and Residual Gravity on Nucleate Pool Boiling Heat Transfer in Microgravity

Yuta FUKUYAMA, Shohei KANAZAWA, Tadashi NAGAYASU, Yasuhisa SHINMOTO, Haruhiko OHTA (Kyushu Univ.), Osamu KAWANAMI (University of Hyogo), Oleg KABOV, Sergey CHIKOV (Int. Heat Transfer Laboratory, Inst. Thermophysics in Novosibirsk), Queeckers PATRICK (Free University of Brussels), Johannes STRAUB (Technical University of Munich)

1. Abstract

Investigation of heat transfer characteristics in nucleate boiling under microgravity condition is essential for the development of the cooling systems handling a large amount of waste heat. To clarify liquid-vapor behaviors and local heat transfer coefficient on the heating surface in microgravity, a transparent heating surface as shown in **Fig.1** was developed. This transparent heating surface has 88 pairs of temperature sensors (1.3mm × 1.3mm) and mini-heaters (3.0mm × 3.0mm) coated directly on the liquid side and the back side, respectively. Pool boiling experiments were conducted during parabolic flight campaign by ESA.

In the present study, based on the detailed analysis of distribution of local heat transfer coefficients, the variations of local boiling heat transfer characteristics are discussed relating to the effect of liquid subcooling and residual gravity.

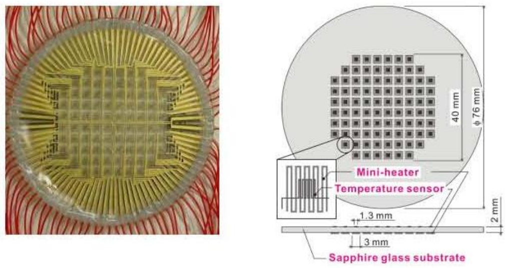

Fig.1 Transparent heating surface

1) Y. Sato, K. Inoue and H.Ohta, J. Jpn. Soc Microgravity Appl, 24, (2007), **71**.

液滴回転法を用いた高温金属融体の表面張力測定

○今井済(学習院大学)，石川毅彦(JAXA)，岡田純平(JAXA)，Vijayu KUMAR(JAXA),
渡邉匡人(学習院大学)，　水野彰敏(学習院大学)

Surface tension measurement of refractory metals by drop rotation method

Wataru IMAI, Takehiko ISHIKAWA, Junpei OKADA, Vijayu KUMAR, Masashito WATANABE, Akitoshi MIZUNO

1. Introduction

Purpose of this study is to measure surface tension of highly viscous materials at high temperature, which is difficult to measure with oscillation method, by rotating levitated droplets. It is known that shape of levitated droplet changes from axis symmetry to non axis symmetry when its rotation rate exceeds a critical value. We build a method by measuring the critical rotating frequency with high accuracy.

2. Experimental method

The experiment was conducted using an electrostatic levitation method in high vacuum. The levitated sample using Coulomb force is molten by heating lasers, and rotated by the rotating magnetic field generated by four coils. Rotating sample is shown in **Fig.1**. The surface tension is measured by measuring rotating frequency at the **Fig.1** (d).

The details of equipment and preliminary experiment are reported in the poster.

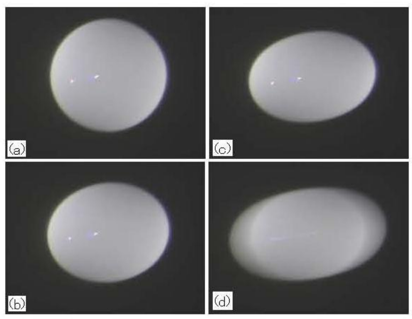

Fig. 1 Side view of a rotating Zr drop : The angular momentum was increased. (a) is axis symmetry, and (d) is closely landed on the bifurcation point.

References

1) BROWN.R, A. & SCRIVEN.L, E. The shape and stability of rotating liquid drops: Proc. R. SOC. Lond. A 371, 331-357(**1980**)
2) W-K, RHIM and T, ISHIKAWA. Noncontact surface tension measurement by drop rotation: The American Institute of Physics. Vol72, No.9, 3572-3576(**2001**)

「きぼう」での強制流動沸騰実験に用いる実験装置の開発

○廣川智己，馬場宗明，新本康久，大田治彦(九州大学)，浅野等(神戸大学)，河南治(兵庫県立大学)，鈴木康一(山口東京理科大学)，今井良二 (IHI)，榎戸一典，豊島悠輝 (有人宇宙システム)，岡　利春，中川陽子，宇宿功史郎(IHI エアロスペース)，木暮和美(日本宇宙フォーラム)，大久保堅剛，松本聡，川崎春夫，澤田健一郎，栗本卓，駒崎雅人，藤井清澄(宇宙航空研究開発機構)

Development of Apparatus for Flow Boiling Experiments to be Performed onboard “KIBO”

Tomoki HIROKAWA, Soumei BABA, Yasuhisa SHINMOTO, Haruhiko OHTA (Kyushu Univ.), Hitoshi ASANO (Kobe Univ.), Osamu KAWANAMI (Univ. of Hyogo), Koichi SUZUKI (Tokyo Univ. of Science, Yamaguchi), Ryoji IMAI (IHI Corp.), Kazunori ENOKIDO, Yuuki TOYOSHIMA (Japan Manned Space Systems Corp. (JAMSS)), Toshiharu OKA, Yoko NAKAGAWA, Koshiro USUKU (IHI Aerospace Co., Ltd. (IA)), Kazumi KOGURE (Japan Space Forum (JSF)), Kengoh OHKUBO, Satoshi MATSUMOTO, Haruo KAWASAKI, Kenichiro SAWADA, Takashi KURIMOTO, Masahito KOMASAKI, Kiyosumi FUJII (Japan Aerospace Exploration Agency (JAXA))

1. Abstract

Recent increase in the size of space platforms requires a capacity to handle a large amount of waste heat. Thermal management systems in space using flow boiling attract much attention because of its superior heat transfer characteristics. However, heat transfer characteristics of boiling and two-phase flow under microgravity conditions are not clarified in detail. Most of existing experiments show only the unsteady state data because of the limitation of microgravity duration. In this research, experiments for boiling and two-phase flow onboard ISS are to be performed under the long term and high quality microgravity conditions. One of important objectives is to produce reliable data useful for future cooling system in space platform. Ground experiments are conducted to verify the performance of the test loop and integrated individual components before their final design for ISS experiments.

Preliminary ground experiments are performed under the similar conditions to those for the ISS experiment. Two different heating methods are examined. One is a step heating and the other is a continuous heating. The heat flux is kept at constant until the steady state is established in the step heating, while, in the continuous heating, the heat flux is increased or decreased at a certain rate to obtain the data similar to that for the steady state within allowable errors. Ground experiments are conducted to verify the agreement of the data obtained by the different methods.

熱フィラメント CVD 法を用いた高重力環境下でのダイヤモンド合成における予備実験

○西村遼 (帝京科学大学)，稲富裕光 (ISAS / JAXA)，高木喜樹 (帝京科学大学)

Preliminary Experiment of Diamond Synthesis with HFCVD under High Gravity Environment

Ryo NISHIMURA [1], Yuko INATOMI [2], Yoshiki TAKAGI[1]

[1]Teikyo University of Science and Technology, [2]ISAS / JAXA

The purpose of this study is to investigate a high gravity effect in diamond synthesis with hot filament chemical vapor deposition (HFCVD) on a centrifuge. We already reported diamond synthesis with graphite rod heating under high gravity[1)], and we suggested that nucleation density of diamond particles were increased with increasing gravity.

In this study, we tried to perform high gravity experiments with a centrifuge for diamond synthesis by HFCVD under 300 and 600 Torr as total pressure. The reaction chamber was mounted on the centrifuge in Japan Aerospace Exploration Agency[2)]. Each experimental condition was as follows: tungsten filament was placed 1.0 mm above the silicon substrate, substrate temperature was around 710°C, reaction time was 20 minutes, and the initial total pressure were 300 Torr (1 Torr for carbon source, and 299 Torr for hydrogen) or 600 Torr (5 Torr for carbon source, and 595 Torr for hydrogen).

Diamond particles were successfully synthesized with the present study. Figure 1 shows SEM photographs of diamond particles with gravity condition under 300 Torr and 600 Torr as total pressure. Nucleation density in 1.6 g_0 experiment (**Fig. 1** (b)) was increased compared with that in 1.0 g_0 experiment (**Fig. 1** (a)) under 300 Torr. However, we found significant difference between 1.0 g_0 and 1.6 g_0 under 600 Torr as total pressure in the high gravity experiments (**Fig. 1** (c) and (d)). We will report the details of the present experiments in the meeting.

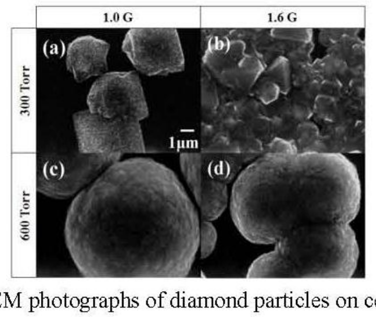

Fig. 1 SEM photographs of diamond particles on centrifuge.

References

1) H. Kageyama, S. Hirai, Y. Takagi and Y. Abe: Journal of the Japan Society of Microgravity Application, **28** (2011) S78.
2) Y. Inatomi, O. Kitafima, W. Huang, K. Kuribayashi and Y. Sawada: Crystal Research and Technology, **32** (1997) 947.

地上および微小重力場における強制対流沸騰熱伝達と気液挙動 -ISS 実験に向けて-

○山口祐太，猿渡賢治，河南治（兵庫県大），浅野等（神戸大），新本康久，大田治彦（九州大），
藤井清澄，駒崎正人，栗本卓（JAXA）

Flow Boiling Heat Transfer and Flow behavior in Terrestrial and Microgravity -Toward ISS Experiment-

Yuta YAMAGUCHI, Kenji SARUWATARI, Osamu KAWANAMI (Univ. Hyogo),
Hitoshi ASANO (Kobe Univ.), Yasuhisa Shinmoto, Haruhiko Ohta (Kyushu Univ.), Kiyosumi FUJII,
Masahito KOMASAKI and Takashi KURIMOTO (JAXA)

1. Introduction

Boiling and two-phase flow is extremely useful method for heat management system in space because it has high heat transfer rate. However, boiling phenomena in microgravity is not clear until now. Japanese research group including authors is planning boiling and two-phase flow experiments utilizing a long-term microgravity environment onboard ISS "KIBO". In this experimental loop, the transparent heated test section is set up for one of the evaporation part. In this paper, we report that current status of the development of the transparent heated tube test-section.

2. Experiment and Results

Fig. 1 shows the result of boiling experiments taken by the transparent heated tube (I.D.= 4 mm, Heated length = 50 mm), which will be used for ISS experiment. The heated transfer coefficients and inner wall temperature coincided with a change in void fraction of the entire of the heated tube.

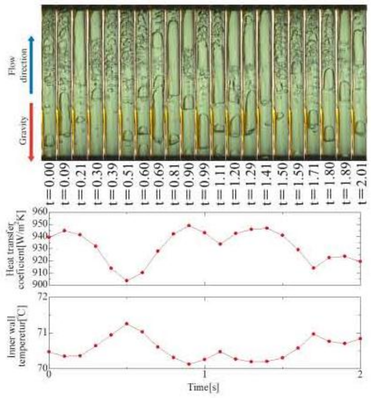

Fig. 1 Flow images and innerwall temperature data (G=50kg/m^{2}s, T_{sub}= 10K, q_w =21.5kW/m^2,vertical flow).

静磁場印加電磁浮遊法による高温融体熱物性計

○ 村井健多太郎，荒川葵，小野寺健太，小山達也，水野章敏，渡邉匡人 (学習院大学),
福山博之（東北大学多元研）

Thermophysical Properties Measurement of High-Temperature Liquids by Electromagnetic Levitation Technique Combined with Static Magnetic Fields

Kentaro MURAI, Aoi ARAKAWA, Kenta ONODERA, Tatsuya KOYAMA, Akitoshi MIZUNO, Masahito WATANABE (Gakushuin Univ.), Hiroyuki FUKUYAMA (IMRAM, Tohoku Univ.)

1. Introduction

Microgravity conditions have advantages of measurement of thermophysical properties, density, viscosity, surface tension, and thermal conductivity etc, of high-temperature liquids by using an electromagnetic levitation (EML) device. Density of the liquid state is very important thermophysical properties for process simulations because the density decides the flow of liquid phases. Thus, many measurements of density have been reported by using various techniques. The EML technique has large advantages for maintaining liquids in a supercooling state and for maintaining the high temperature state with keeping high purity of measurement samples due to the containerless environment. For determine the density, we must also precisely measure the mass of samples. During long time levitation in high temperature regions, the sample mass changed by evaporations. Thus, we must reduce observation time of liquid droplet motion for precise density measurements. For this requirement, we applied the technique of the static magnetic field applied EML for density measurements [1,2].

2. Experiments and Results

For applying the technique to the density measurements, we specially designed EML coils in order to suppress the deformation of droplet shape in 8T magnetic fields. Using these techniques, we measured the density of various Cu-based alloys liquids with reduction of uncertainty of measurements to the order of magnitude compared with previously reported data by conventional EML technique. My poster presentation focuses on the density variation of the immiscible alloy liquids of Cu-Co alloys with various compositions.

References

1) H. Kobatake *et al.*, Meas. Sci. Technol., 21 (2010) 025901.

2) M. Watanabe *et al.*, Faraday Discuss., 136 (2007) 279-285.

SI, Ge における無容器過冷凝固

○石橋裕輔，米山覚，永山勝久，栗林一彦

Containerless Solidification of Si and Ge into Undercooled Melt

Yusuke ISHIBASHI, Satoru YONEYAMA, Katsuhisa NAGAYAMA, Kazuhiko KURIBAYASHI
(Shibaura Institute of Technology)

1. Abstract

In recent years, with advances in levitation techniques, the research on undercooled melt has brought a new insight on the kinetics of rapid solidification. Using this technique, we performed the containerless crystallization of Si and Ge. Experimental results showed that the interface morphology of the crystallized Si and Ge was quite different from those of metals and alloys. That is, it respectively looks like plate-like crystals and facetted dendrites at low undercooling and medium undercooling. Although the range of the undercooling differs in Si and Ge, the growth velocities are fundamentally scaled by the thermal diffusivities and the temperature increase caused by the release of the latent heat. This result means that the growth velocity can be expressed by the product of the thermal diffusivity and the growth kinetics. Microscopic observation of the dendrite morphologies revealed that the kinetics of crystal growth in low and medium undercooling is represented by two-dimensional nucleation at the reentrant corner formed at the edge of the two parallel twins. On the other hand, at high undercooling, the interface attachment kinetics controlled by thermal diffusion which is described by a modified Wilson-Frenkel model dominates the growth velocity.

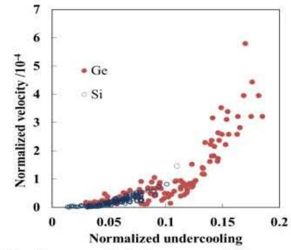

Fig.1 Relation between dimensionless growth velocity and dimensionless undercooling, which are normalized by the thermal diffusive speed α/a and the temperature increase due to the release of latent heat ΔHf/CP. Open and closed circles are for Si and Ge.

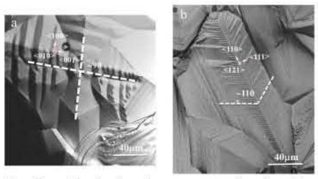

Fig.2 Typical images of facetted dendrites in Ge samples: (a) containerlessly solidified at ΔT = 151 K showing <100>dendrite and (b) solidified by dropping onto the optically polished silicon plate at the equilibrium melting temperatures showing <110>dendrite. Each image was taken by laser scanning microscopy.

References

1) Y. Ishibashi, K. Kuribayashi, K. Nagayama: JOM, **64** (2012), pp. 1102-1108

無容器プロセスによるマルチフェロイック材料の創製

○大内良晃，高杉茉里，栗林一彦，永山勝久 (芝浦工業大学)，M.S.Vijaya Kumar (JAXA)

Formation of Multiferroic Materials by Means of Containerless Processing

Yoshiaki OOUCHI, Mari TAKASUGI, Kazuhiko KURIBAYASHI, Katsuhisa NAGAYAMA
(Shibaura Institute of Technology) and M.S.Vijaya Kumar (JAXA)

1. Abstract

The term multiferroism has been coined to describe materials in which two or all three of ferroelectricity, ferromagnetism and ferroelasticity occur in the same phase. Particularly the coupling between ferroelectricity and ferromagnetism has been expected to form a new material which can posses a function as a storage medium based on the new concept that the electric polarization can be controlled by a magnetic field and the spin alignment by the electric field. Hexagonal $RMnO_3$ (R = rare-earth element) with a space group of $P6_3cm$ has been cited as a strong candidate for the multiferroic material. However the materials for practical applications have not been developed because the material shows antiferromagnetism, which means the magnetic moment disappears as a whole, and also shows a low magnetic transition temperature less than 100K.

From these points of view, we considered that the composite of the ferroelectric phase and ferromagnetic phase with using Fe^{3+}, the magnetic moment of which is larger than that of Mn^{3+}, are realistic to show the multiferroism. According to this idea, utilizing the containerless technique we attempted to synthesize a multiferroic composite of a metastable hexagonal $RFeO_3$ phase (h-$RFeO_3$) which shows ferroelectricity and magnetite (Fe_3O_4) which shows ferromagnetism. As a result, we reached the conclusion that $Lu(Fe_xMn_{1-x})_{2+y}O_{4+z}$ is one of the potential materials with multiferroism, because the substitution of a small fraction of Fe^{3+} to Mn^{2+} stabilizes the metastable h-$LuFeO_3$, and suppresses the precipitation of the equilibrium orthorhombic phase (o-$LuFeO_3$).

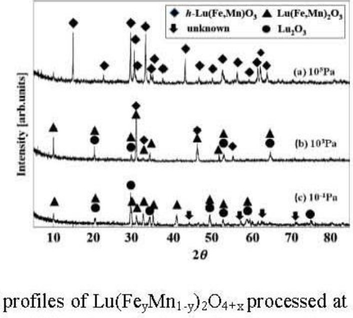

Fig. 1. XRD profiles of $Lu(Fe_yMn_{1-y})_2O_{4+x}$ processed at various oxygen partial pressure (PO_2). As indicated in this figure the sample processed at 10^5Pa of PO_2 distinctly shows the pattern of $_h$-$RFeO_3$.

Si の過冷凝固に及ぼす Sn の影響

○米山　覚、永山　勝久 (芝浦工業大学)、栗林　一彦 (芝浦工業大学)

Rapid Solidification of Levitated and Undercooled Si-Sn Alloy Melt

Satoru Yoneyama[1], Katsuhisa Nagayama[1] , Kazuhiko Kuribayashi[1]

[1] Department of Materials Science and Engineering.

Shibaura Institute of Technology

3-7-5 Toyosu, Koto-ku, Tokyo 135-8548, Japan

In order to manufacture spherical crystals of Si, containerless solidification, where the melt is levitated and solidified without using a crucible, has been carried out. Until now, this process has been analyzed on the basis of the dendrite growth model proposed by Lipton, Kurz and Trivedi (LKT model). However, it is unreasonable to apply this model to semiconductors, because in the LKT model, the crystal-melt interface is assumed to be rough. In the present investigation the containerless crystallizing of Sn doped Si was performed and the influence of alloying on the solidification kinetics was analyzed.

From the point of morphologies of the solid-liquid interface the solidification behavior was approximately classified into three regions as similar as in Si. That is, ΔT<80K is low undercooling, 80K< ΔT<160K is medium undercooling and ΔT>160K is high undercooling, although the plate-like needle crystal which appears at low undercooling is slightly different from that of pure Si: the plate-like crystal looks as if it has been fragmented into small pieces being different from that of pure Si. **Figure 1** shows the faceted dendrite which appeared on the surface of the sample solidified at low undercooling. It was found that the facetted dendrite preferentially grows in the <110> direction. Compared with pure Si, <100> dendrites drastically decreased. The reason for this discrepancy is discussed on the basis of the relation with the growth velocities.

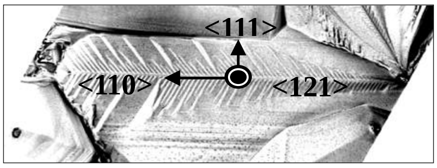

Fig. 1 Photograph of faceted dendrite taken by a laser scanning microscope.